

UNCLASSIFIED

AD NUMBER

AD205010

CLASSIFICATION CHANGES

TO: **unclassified**

FROM: **confidential**

LIMITATION CHANGES

TO:

**Approved for public release, distribution
unlimited**

FROM:

**Distribution authorized to U.S. Gov't.
agencies and their contractors;
Administrative/Operational Use; FEB 1955.
Other requests shall be referred to David
Taylor Model Basin, Washington, DC.**

AUTHORITY

**USNRDC ltr, 15 Mar 1971; USNRDC ltr, 15
Mar 1971**

THIS PAGE IS UNCLASSIFIED

UNCLASSIFIED

A 2050 00
D 2050 00

Armed Services Technical Information Agency

ARLINGTON HALL STATION
ARLINGTON 12 VIRGINIA

CODE
23

FOR
MICRO-CARD
CONTROL ONLY

1 OF 1

NOTICE: WHEN GOVERNMENT OR OTHER DRAWINGS, SPECIFICATIONS OR OTHER DATA
ARE USED FOR ANY PURPOSE OTHER THAN IN CONNECTION WITH A DEFINITELY RELATED
GOVERNMENT PROCUREMENT OPERATION, THE U. S. GOVERNMENT THEREBY INCURS
NO RESPONSIBILITY, NOR ANY OBLIGATION WHATSOEVER; AND THE FACT THAT THE
GOVERNMENT MAY HAVE FORMULATED, FURNISHED, OR IN ANY WAY SUPPLIED THE
SAID DRAWINGS, SPECIFICATIONS, OR OTHER DATA IS NOT TO BE REGARDED BY
IMPLICATION OR OTHERWISE AS IN ANY MANNER LICENSING THE HOLDER OR ANY OTHER
PERSON OR CORPORATION, OR CONVEYING ANY RIGHTS OR PERMISSION TO MANUFACTURE,
SELL, USE, OR OTHERWISE EXPLOIT THE SAME, WHICH MAY BE RELATED THERETO.

**Best
Available
Copy**

AD 205010

UNCLASSIFIED

LINEARIZED THEORY FOR FLOWS ABOUT LIFTING FOILS AT ZERO
CAVITATION NUMBER

by

M.P. Tulin and M.P. Burkart

"This document contains information affecting the national defense of the United States within the meaning of the Espionage Laws, Title 18, U.S.C., Sections 793 and 794. The transmission or the revelation of its contents in any manner to an unauthorized person is prohibited by law."

"Reproduction of this document in any form by other than naval activities is not authorized except by special approval of the Secretary of the Navy or the Chief of Naval Operations as appropriate."

February 1955

Report C-638
NS 715-102

UNCLASSIFIED

UNCLASSIFIED

ii

TABLE OF CONTENTS

	Page
ABSTRACT	1
INTRODUCTION.....	1
LINEARIZED THEORY	2
THE HYDROFOIL-AIRFOIL EQUIVALENCE	5
THE FLAT-PLATE HYDROFOIL	9
THE FLAPPED-PLATE HYDROFOIL	10
LOW-DRAG HYDROFOILS.....	12
SUMMARY	16
APPENDIX A - USEFUL RESULTS OF THE LINEARIZED AIRFOIL THEORY....	19
APPENDIX B - WAKE SHAPE ACCORDING TO LINEARIZED AND EXACT THEORY.....	20
Linearized Theory	20
Exact Theory.....	22
APPENDIX C - LISTING OF USEFUL THEORETICAL RESULTS	24
REFERENCES	25

UNCLASSIFIED

UNCLASSIFIED

iii

NOTATION

- A_0 The Fourier coefficient of zero order = $-\frac{1}{\pi} \int_0^{\pi} \frac{d\bar{y}_0}{ds}(\theta) d\theta$
 A_n The Fourier coefficient of nth order = $\frac{2}{\pi} \int_0^{\pi} \frac{d\bar{y}_0}{ds}(\theta) \cos n\theta d\theta$
 a, b Constants
 C_D Drag coefficient = $\frac{D}{\frac{1}{2} \rho U_{\infty}^2 s}$
 C_L Lift coefficient = $\frac{L}{\frac{1}{2} \rho U_{\infty}^2 s}$
 C_{L_d} Design lift coefficient
 C_M Moment coefficient = $\frac{M}{\frac{1}{2} \rho U_{\infty}^2 s^2}$
 C_{M_3} Third moment coefficient = $\frac{M_3}{\frac{1}{2} \rho U_{\infty}^2 s^2}$
 D Drag
 L Lift
 M First moment about the leading edge
 M_3 Third moment about the leading edge
 p Local static pressure
 p_{∞} Static pressure of stream at infinity
 p_c Cavity pressure
 s Body chord length
 s' Dummy variable
 t Dummy variable
 U_{∞} The uniform velocity at ∞ , parallel to the x -axis
 u The x -component of the perturbation velocity
 \vec{v} The velocity of the fluid at any point in the flow field = $\vec{U}_{\infty} + \vec{v}$

(10) (15)

UNCLASSIFIED

iv

v	The y-component of the perturbation velocity
\dot{v}	The perturbation velocity
s	A space coordinate parallel to U_∞
s'	Dummy variable
x_b	The length of the fixed portion of a flapped-plate hydrofoil
y	A space coordinate measured normal to the z-direction
z	A complex variable, $z = x + iy$
α	Operating angle of attack measured from the direction of z
α'	The difference between the operating angle of attack and the design angle of attack
$\delta(z)$	The Dirac delta function
ϵ	The flap angular deflection for the flapped-plate hydrofoil
ζ	A complex variable, $\zeta = \xi - iq$
ζ_1	A parameter
η	The imaginary coordinate in the complex ζ -plane
θ	A parameter defined on the airfoil: $\frac{\bar{x}}{s} = \frac{1}{2}(1 - \cos \theta)$
η	A parameter defined for the flapped-plate hydrofoil, $\sqrt{\frac{s_b}{s}} = \frac{1}{2}(1 - \cos \theta_A)$
v	The complex velocity, $v = u - i\dot{v}$
ξ	The real coordinate in the complex ζ -plane
ρ	The constant fluid density
σ	Cavitation number = $\frac{P_\infty - P_c}{\frac{1}{2}\rho U_\infty^2}$
ϕ	Perturbation velocity potential such that $\dot{v} = i\phi$
Subscript s	Indicates quantities determined on the body surface
Subscript c	Indicates quantities determined on the cavity surface
Unbarred symbols	refer to cavity flow, Figure 1
Barred symbols	refer to non-cavity flow, Figure 2
O	symbolizes "order of"

UNCLASSIFIED

UNCLASSIFIED

ABSTRACT

A linearized theory is developed for steady, two-dimensional cavity flows about hydrofoil sections at zero cavitation number. The problem of calculating the flow characteristics including the hydrofoil forces and pitching moments is reduced to an equivalent problem of the classical thin airfoil theory. This equivalence is used to investigate the characteristics of hydrofoil shapes of practical importance. In particular, the lift, drag, and pitching moment due to angle of attack and flap deflection are determined. The important effect of hydrofoil shape on the cavitation drag is revealed, and a family of moderately low drag sections is specified.

The linearized theory results for the flat plate are shown to be equal to the first-order (in angle of attack) terms of the exact theory results.

INTRODUCTION

With the increasing speeds of naval vessels and underwater missiles, effects of cavitation become increasingly important. For sufficiently high speeds, the design of propellers, plane control surfaces, and main supporting foils requires information regarding the forces and moments developed on lifting surfaces with fully developed, trailing cavities. For surfaces of moderate aspect ratio with sufficiently long cavities, much of the necessary design information would be obtained from studies of two-dimensional hydrofoils operating at zero cavitation number, that is, with a pressure in the cavity equal to the pressure of the undisturbed stream. Such a study, utilizing a first-order approximation linearized theory, comprises the content of the present paper.

The actual problem being considered here may be stated in the following way: To find the lift, drag, and pitching moment about the leading edge, of two-dimensional sections immersed at an angle of attack, in a uniform, infinite, steady, inviscid stream for which it is assumed that cavitation occurs when the fluid pressure on the surface of the body becomes equal to the pressure of the undisturbed stream. For such a flow, the cavity extends to infinity. The hydrofoil sections are assumed to be of almost arbitrary shape; the only specifications are that (a) they have sharp trailing edges and sufficiently sharp noses so that cavitation occurs at both the leading and trailing edges, (b) the section is sufficiently thin so that its upper surface lies completely within the cavity which springs from the leading edge and thus does not play a role in the determination of the flow pattern, and (c) the slopes and curvatures of the sections' bottoms are sufficiently small to allow meaningful results to be obtained from the linearized theory. Although the problem is considered for all sections meeting the above specifications, the derived results are physically meaningful only for those sections for which the derived pressures on the bottom surface are nowhere less than the pressure of the stream at infinity.

UNCLASSIFIED

Earlier mathematical investigations which are pertinent to the present problem (see Reference 1, Chapter II) are almost all concerned with exact solutions. Of that work which is not mainly concerned with mathematical existence and uniqueness questions, the work of Levi-Civita is particularly of interest; see Chapter XII of Reference 2 for an excellent discussion. Levi-Civita considers an inverse problem and obtains results which allow the construction of flows like those considered here, but without initial specification of the hydrofoil shape. With regard to the practical solution of the present problem, there has been little progress beyond Levi-Civita's work. As far as exact solutions in closed form are concerned, then, the general direct problem, which is nonlinear in nature, remains unsolved. This fact suggests the derivation of approximate theory. Considering the nature of the configurations involved, a first-order linearized theory identical in its approximations to the now classical thin airfoil theory, and similar to the linearized theory already developed for symmetric, two-dimensional cavity flows (see Reference 3), seems especially appropriate.

LINEARIZED THEORY

It will be useful to consider both the linearized version of the present cavitation problem and the classical problem of thin airfoil theory, for which the solution has long been known.

Thus, consider the flows schematically illustrated in Figures 1 and 2, and let

- \hat{v} = velocity of fluid at any point in the free field, = $\hat{U}_\infty + \hat{v}$
- \hat{v} = perturbation velocity,
- x, y = x and y components, respectively, of \hat{v} ,
- \hat{U}_∞ = uniform velocity at ∞ , parallel to the x axis,
- p = local static pressure,
- p_∞ = static pressure of stream at infinity,
- p_c = cavity pressure,
- σ = cavitation number = $\frac{p_\infty - p_c}{\frac{1}{2} \rho \hat{U}_\infty^2}$,
- ρ = constant fluid density,
- ϕ = perturbation velocity potential such that $\hat{v} = \nabla \phi$.

Subscript 0 indicates quantities determined on the body surface,

Subscript c indicates quantities determined on the cavity surface,

Unbarred symbols refer to the cavity flow, Figure 1,

Barred symbols refer to the nearcavity flow, Figure 2,

O symbolizes "order of."

CONFIDENTIAL

3

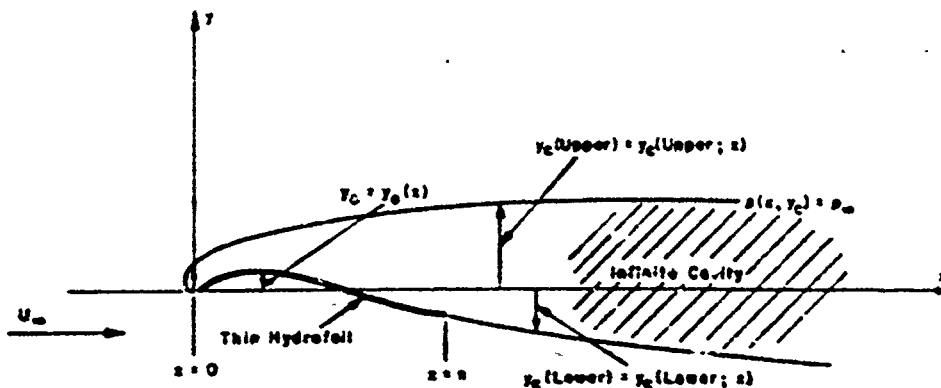


Figure 1 - Schematic Cavity Flow $\sigma = 0$

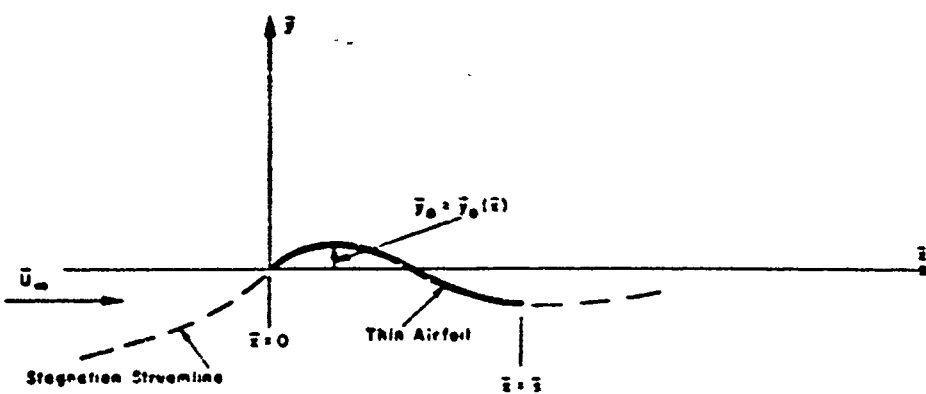


Figure 2 - Schematic Noncavity Flow ($\sigma = \infty$)

On the bottom of the hydrofoil, the streamline slope is specified by

$$\frac{dy_0}{dz}(z) = \frac{v(z, y_0)}{U_\infty + v(z, y_0)} = \frac{\sigma(z, y_0)}{U_\infty} \left[1 - \frac{u(z, y_0)}{U_\infty} + O\left(\frac{u(z, y_0)^2}{U_\infty}\right) \right] \quad [1]$$

On the airfoil, the streamline slope is specified on the top by

$$\frac{d\bar{y}_0(\bar{z})}{d\bar{z}} = \frac{\bar{v}(\text{upper}; \bar{z}, \bar{y}_0)}{\bar{U}_\infty} \left[1 - \frac{\bar{u}(\text{upper}; \bar{z}, \bar{y}_0)}{\bar{U}_\infty} + O\left(\frac{\bar{u}(\text{upper}; \bar{z}, \bar{y}_0)^2}{\bar{U}_\infty}\right) \right]$$

and on the bottom by

$$\frac{d\bar{y}_0(\bar{z})}{d\bar{z}} = \frac{\bar{v}(\text{lower}; \bar{z}, \bar{y}_0)}{\bar{U}_\infty} \left[1 - \frac{\bar{u}(\text{lower}; \bar{z}, \bar{y}_0)}{\bar{U}_\infty} + O\left(\frac{\bar{u}(\text{lower}; \bar{z}, \bar{y}_0)^2}{\bar{U}_\infty}\right) \right]$$

CONFIDENTIAL

CONFIDENTIAL

4

On the wall of the hydrofoil's cavity, the static pressure and thus the cavitation number are specified. From Bernoulli's equation it follows that

$$\sigma = \frac{2u(z, y_c)}{U_\infty} + O\left(\frac{u(z, y_c)}{U_\infty}\right)^2 = \text{constant} \quad [3]$$

It may be inferred from the Cauchy-Riemann equations that the perturbation velocity changes very slowly in space if streamline slopes and curvatures are small, so that some justification exists for satisfying linearized boundary conditions on the x - (or \bar{x} -) axis instead of on the thin bodies. At this point it is not profitable to attempt further to justify the approximations involved in the linearization, but rather to provide further justification thru a comparison that will finally be made between exact and linearized results for a particular case (pages 9 and 10).

The linearized boundary conditions become

$$\frac{dy_0}{dx}(z) = \frac{u(z, 0-)}{U_\infty} = \frac{1}{U_\infty} \frac{\partial \phi}{\partial y}(z, 0-); \quad 0 < z < s \quad [1a]$$

$$\sigma = 0 = \frac{2u(z, 0-)}{U_\infty} = \frac{2}{U_\infty} \frac{\partial \phi}{\partial x}(z, 0-); \quad z > s \quad [3a]$$

$$\sigma = 0 = \frac{2u(z, 0+)}{U_\infty} = \frac{2}{U_\infty} \frac{\partial \phi}{\partial x}(z, 0+); \quad z > 0$$

$$\frac{d\bar{y}_0}{d\bar{x}}(\bar{x}) = \frac{\bar{u}(\bar{x}, 0)}{\bar{U}_\infty} = \frac{1}{\bar{U}_\infty} \frac{\partial \bar{\phi}}{\partial \bar{y}}(\bar{x}, 0); \quad 0 < \bar{x} < \bar{s} \quad [2a]$$

Finally, then, the linearized problems may be stated: To find the harmonic functions $\phi(z, y)$ and $\bar{\phi}(\bar{x}, \bar{y})$, whose gradients in the limit vanish everywhere on a circle of sufficiently large radius about the origin, which satisfy the boundary conditions of Equations [1a], [2a], [3a] (which are incorporated in Figures 3 and 4) and which, for the sake of physical reality, produce smooth flow at the points $(s, 0-)$ and $(\bar{s}, 0)$. In Figure 4, the asymmetry of $\bar{\phi}(\bar{x}, \bar{y})$, which follows from the definition of $\bar{\phi}(\bar{x}, \bar{y})$ just given, is used to specify boundary conditions on the entire \bar{x} -axis.

The problem for $\bar{\phi}(\bar{x}, \bar{y})$ is essentially solved through the observation that its boundary conditions may be satisfied by a suitable distribution of vortex singularities placed on the interval $0 < \bar{x} < \bar{s}$. The strength of the distributed vortex singularities is proportional to $\bar{u}(\bar{x}, 0+)$. An integral equation is then obtained which relates $\bar{u}(\bar{x}, 0+)$ to the airfoil shape. It is

$$\bar{u}(\bar{x}, 0) = \bar{U}_\infty \frac{dy_0}{d\bar{x}}(\bar{x}) = \frac{1}{\pi} \int_0^{\bar{s}} \frac{\bar{u}(\bar{x}', 0+)}{\bar{x}' - \bar{x}} d\bar{x}' \quad [4]$$

CONFIDENTIAL

CONFIDENTIAL

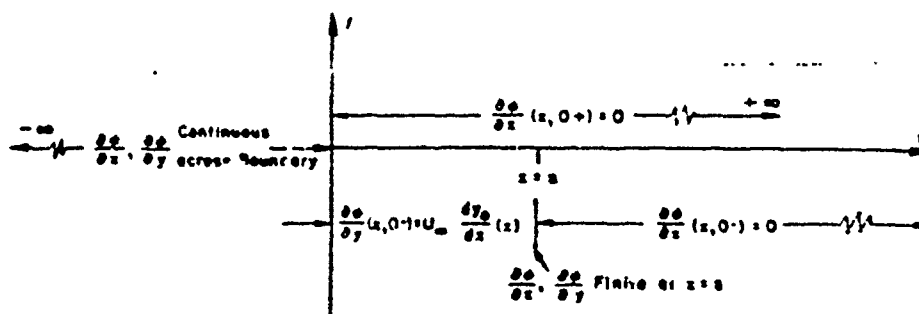
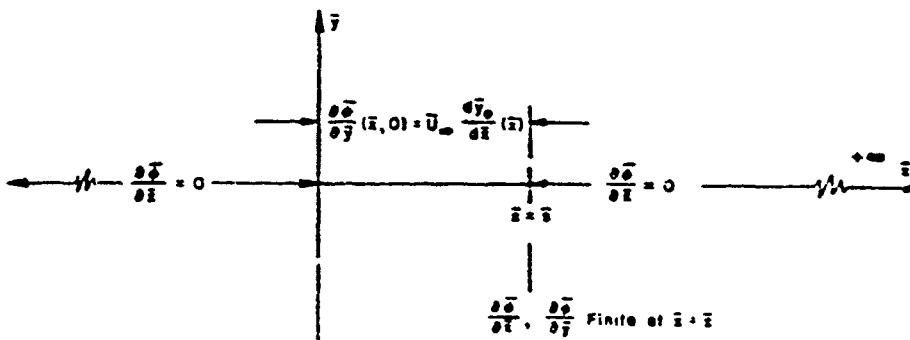
Figure 3 - The Linearized Boundary Conditions for a Cavitating Hydrofoil, $\sigma = 0$ 

Figure 4 - The Linearized Boundary Conditions for an Airfoil. No Cavitation.

The integral Equation [4] is conveniently solved by Glauert's method (see Reference 4, Chapter VII). Useful results of the solution are collected for reference in Appendix A.

THE HYDROFOIL-AIRFOIL EQUIVALENCE

It is now to be shown that for every cavitating hydrofoil problem of the type just described, an intimately related thin airfoil problem exists whose solution may readily be converted into the solution of the hydrofoil problem.

First, recall that the complex velocity is an analytic function of the complex space coordinate:

$$u(z, y) - i\tau(z, y) = f(z + iy) = f(z)$$

and that the function $y(\zeta)$ created from $f(z)$ by a conformal transformation of the z -space to a new, say, ζ -space is also a complex velocity.

Then consider the transformation

$$\sqrt{z} = -\zeta = -(\zeta + i\eta) \quad [5]$$

CONFIDENTIAL

CONFIDENTIAL

6

which transforms the top of the positive x -axis into the negative ζ -axis, the bottom of the positive x -axis into the positive ζ -axis, and the entire x -plane, exclusive of the cut, positive x -axis, into the lower half of the ζ -plane.

The flow problem, schematically illustrated in Figure 3, is shown as a complex variable problem in the original x -plane in Figure 3, and is shown in the transformed ζ -plane in Figure 6.

It follows from a comparison of Figures 4 and 6, that the problem represented in Figure 3 is exactly a thin airfoil problem. The airfoil equivalent to any given hydrofoil is one such that (using the initial notation for the airfoil flow):

$$\bar{v}(\bar{z}) = v(\bar{z}^2); \quad v(z) = \bar{v}(\sqrt{z})$$

or,

$$\frac{dy_0}{d\bar{z}}(\bar{z}) = \frac{dy_0}{dz}(\bar{z}^2); \quad \frac{dy_0}{dz}(z) = \frac{dy_0}{d\bar{z}}(\sqrt{z})$$

$$\bar{u}(\bar{z}) = u(\bar{z}^2); \quad u(z) = \bar{u}(\sqrt{z})$$

[7]

$$\text{and } \bar{U}_\infty = U_\infty$$

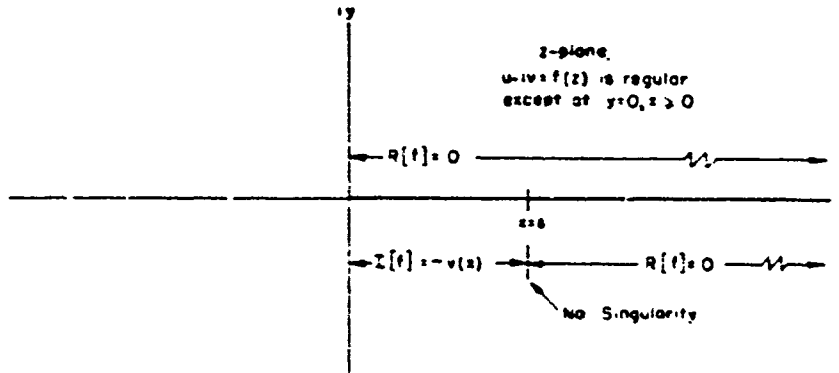


Figure 3 - The Hydrofoil Problem in x -space;

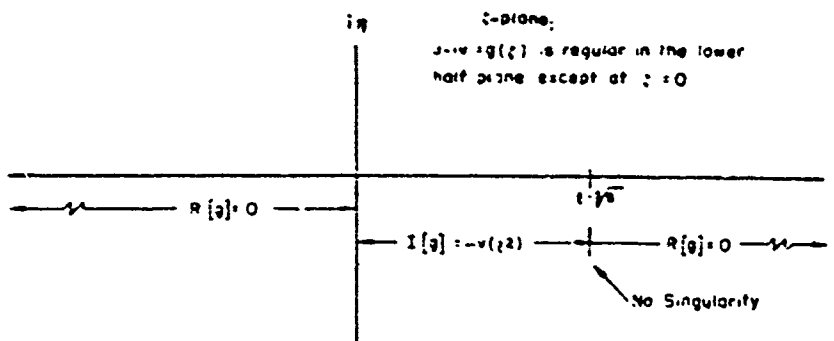


Figure 3 - The Hydrofoil Problem in ζ Space, $\sqrt{z} = -\zeta$

CONFIDENTIAL

CONFIDENTIAL

As examples:

- a. The flat plate hydrofoil of chord s at an angle of attack α , $(dy_0/dx)(x) = -\alpha$, is equivalent to the flat plate airfoil of chord \sqrt{s} at an angle of attack α , $(d\bar{y}_0/d\bar{x})(\bar{x}) = -\alpha$.
- b. The hydrofoil of shape $y_0 = ax + bx^2$, $(0 < x < 1)$, $(dy_0/dx)(x) = a + 2bx$ is equivalent to the airfoil of shape $\bar{y}_0 = a\bar{x} + b\bar{x}^2$, $(0 < \bar{x} < 1)$, $(d\bar{y}_0/d\bar{x})(\bar{x}) = a + 2b\bar{x}^2$.

As a consequence of the hydrofoil-airfoil equivalence, the lift, drag, and pitching moment of a hydrofoil correspond to certain characteristics of the equivalent airfoil.

For the hydrofoil:

$$\text{The lift } L = \int_0^s [p(z, 0-) - p(z, 0+)] dz \quad [8]$$

$$\text{The drag } D = - \int_0^s \frac{dy_0}{dx}(z) [p(z, 0-) - p(z, 0+)] dz \quad [9]$$

The moment M about the leading edge (+ counterclockwise)

$$= \int_0^s z [p(z, 0-) - p(z, 0+)] dz \quad [10]$$

Using the linearized Bernoulli equation and nondimensionalizing, these expressions become

$$C_L = \frac{L}{\frac{1}{2} \rho U_\infty^2 s} = - \int_0^s \frac{2u(z, 0-)}{s U_\infty} dz \quad [8a]$$

$$C_D = \frac{D}{\frac{1}{2} \rho U_\infty^2 s} = \int_0^s 2 \frac{dy_0}{dx}(z) \cdot \frac{u(z, 0-)}{s U_\infty} dz \\ - \int_0^s \frac{v(z, 0-)}{U_\infty} \cdot \frac{u(z, 0-)}{U_\infty} dz \quad [9a]$$

$$C_M = \frac{M}{\frac{1}{2} \rho U_\infty^2 s^2} = - \int_0^s \frac{2z}{s^2} \frac{u(z, 0-)}{U_\infty} dz \quad [10a]$$

These coefficients may be expressed in terms of quantities in the airfoil plane:

$$C_L = - \int_0^{\sqrt{s}} \frac{4\bar{z}\bar{v}(\bar{z}, 0-)}{s U_\infty} d\bar{z} \quad [3a]$$

CONFIDENTIAL

CONFIDENTIAL

8

$$C_D = \int_0^{\sqrt{s}} 4\bar{z} \frac{\bar{u}(\bar{z}, 0-) \bar{u}(\bar{z}, 0+)}{s U_\infty^2} d\bar{z} \quad [9b]$$

$$C_M = - \int_0^{\sqrt{s}} \frac{4\bar{z}^3 \bar{u}(\bar{z}, 0-)}{s^2} d\bar{z} \quad [10b]$$

The expression for the drag coefficient may be further reduced by using the result contained in Equation [4]:

$$C_D = - \int_0^{\sqrt{s}} \frac{4\bar{z}\bar{u}(\bar{z}, 0-)}{s^2 U_\infty^2} d\bar{z} \int_0^{\sqrt{s}} \frac{\bar{u}(\bar{z}', 0-)}{\bar{z}' - \bar{z}} d\bar{z}' = - \int_0^{\sqrt{s}} \frac{4\bar{z}\bar{u}(\bar{z}', 0-)}{s^2 U_\infty^2} d\bar{z}' \int_0^{\sqrt{s}} \frac{\bar{u}(\bar{z}, 0-)}{\bar{z} - \bar{z}'} d\bar{z} \quad [9c]$$

Using the identity $\frac{\bar{z}}{\bar{z} - \bar{z}'} = \frac{\bar{z}'}{\bar{z} - \bar{z}'} + 1$

$$C_D = + \int_0^{\sqrt{s}} \frac{4\bar{z}\bar{u}(\bar{z}', 0-)}{s^2 U_\infty^2} d\bar{z}' \int_0^{\sqrt{s}} \frac{\bar{u}(\bar{z}, 0-)}{\bar{z} - \bar{z}'} d\bar{z} + \int_0^{\sqrt{s}} \frac{4\bar{z}\bar{u}(\bar{z}, 0-)}{s^2 U_\infty^2} d\bar{z} \int_0^{\sqrt{s}} \bar{u}(\bar{z}', 0-) d\bar{z}' \quad [9d]$$

or

$$2\pi C_D = \left[\frac{2}{\sqrt{s} U_\infty} \int_0^{\sqrt{s}} \bar{u}(\bar{z}, 0-) d\bar{z} \right]^2 \quad [9e]$$

For the equivalent airfoil:

$$\text{The lift } L = \int_0^{\sqrt{s}} [\bar{p}(\bar{z}, 0-) - \bar{p}(\bar{z}, 0+)] d\bar{z} \quad [11]$$

The moment \bar{M} about the leading edge (- counterclockwise)

$$= \int_0^{\sqrt{s}} \bar{z} [\bar{p}(\bar{z}, 0-) - \bar{p}(\bar{z}, 0+)] d\bar{z} \quad [12]$$

$$\text{The third moment } \bar{M}_3 = \int_0^{\sqrt{s}} \bar{z}^3 [\bar{p}(\bar{z}, 0-) - \bar{p}(\bar{z}, 0+)] d\bar{z} \quad [13]$$

Again using the linearized Bernoulli equation and nondimensionalizing, these expressions become:

$$\bar{C}_L = \frac{\bar{L}}{\frac{1}{2} s U_\infty^2 \sqrt{s}} = - \int_0^{\sqrt{s}} \frac{4\bar{z}\bar{u}(\bar{z}, 0-)}{\sqrt{s} U_\infty} d\bar{z} \quad [11a]$$

CONFIDENTIAL

CONFIDENTIAL

3

$$\bar{C}_M = \frac{\bar{W}_1}{\frac{1}{2} \rho U_\infty^2 s} = - \int_0^{\frac{s}{2}} \frac{4\bar{x}\bar{u}(\bar{x}, 0)}{s^2 U_\infty} d\bar{x} \quad [12a]$$

$$\bar{C}_{M_3} = \frac{\bar{W}_3}{\frac{1}{2} \rho U_\infty^2 s^2} = - \int_0^{\frac{s}{2}} \frac{4\bar{x}^3 \bar{u}(\bar{x}, 0)}{s^2 U_\infty} d\bar{x} \quad [13a]$$

A comparison of Equations [8b], [10a], and [10b] with Equations [11a], [12a] and [13a] yields the following identities:

$$C_L = \bar{C}_M \quad [14]$$

$$C_M = \bar{C}_{M_3} \quad [15]$$

$$C_D = \frac{1}{8\pi} \bar{C}_L^2 \quad [16]$$

These results, together with Equation [6] which defines the airfoil equivalent to a given hydrofoil, completely accomplish the reduction of the hydrofoil problem to an airfoil problem. They will be used in the following sections to study the characteristics of the supercavitating hydrofoil.

THE FLAT-PLATE HYDROFOIL

The case of the cavitating flat plate at an angle of attack α is particularly interesting since the exact solution has long been known (see Reference 5, Chapter IV) and because it provides information on forces and moments due solely to angle of attack.

The exact results for lift, drag, and pitching moment are:

$$C_L(\text{exact}) = \frac{2\pi \sin \alpha \cos \alpha}{4 + \pi \sin \alpha} = \frac{\pi \alpha}{2} + O(\alpha^3) \quad [17]$$

$$C_M(\text{exact}) = \left(\frac{2\pi \sin \alpha}{4 + \pi \sin \alpha} \right) \left(1 - \frac{3 \cos \alpha}{4(4 + \pi \sin \alpha)} \right) = \frac{5\pi \alpha}{32} + O(\alpha^3) \quad [18]$$

$$C_D(\text{exact}) = C_L(\text{exact}) \cdot \tan \alpha = \frac{\pi \alpha^2}{2} + O(\alpha^3) \quad [19]$$

According to Equation [6], and as has been noted, the flat-plate hydrofoil at angle of attack α is equivalent to a flat-plate airfoil at angle of attack α . It is easily shown, using results of the thin airfoil theory, (see Appendix A) that

$$C_L(\text{linearized}) = \bar{C}_M(\text{linearized}) = \frac{\pi \alpha}{2} \quad [17a]$$

CONFIDENTIAL

CONFIDENTIAL

10

$$C_M(\text{linearized}) = \bar{C}_{M_3}(\text{linearized}) = \frac{5\pi\alpha}{32} \quad [13a]$$

$$C_D(\text{linearized}) = \frac{1}{8\pi} \bar{C}_L^2(\text{linearized}) = \frac{(2\pi\alpha)^2}{8\pi} = \frac{\pi\alpha^2}{2} \quad [19a]$$

The shape of the cavity may also be determined. It is shown in Appendix B that a foil of unit chord:

$$\begin{aligned} y_c(\text{linearized; upper}) &= \alpha \left[-x + \frac{1}{2}(1 + 2\sqrt{x}) \sqrt{x + \sqrt{x}} \right. \\ &\quad \left. + \frac{1}{4} \ln \left(1 + 2\sqrt{x} - 2\sqrt{x + \sqrt{x}} \right) \right], x > 0 \end{aligned} \quad [20]$$

$$\begin{aligned} y_c(\text{linearized; lower}) &= \alpha \left[-x + \frac{1}{2}(2\sqrt{x} - 1) \sqrt{x - \sqrt{x}} \right. \\ &\quad \left. - \frac{1}{4} \ln \left(-1 + 2\sqrt{x} + 2\sqrt{x - \sqrt{x}} \right) \right], x > 1 \end{aligned}$$

and,

$$y_c(\text{exact}) = y_c(\text{linearized}) + O(\alpha^2) \quad [20a]$$

The fact that the linearized theory, as applied here to the case of the flat plate gives results for forces, moments, and cavity shapes that are identical with the leading term in the exact solution expressions for corresponding quantities, is an important justification for the linearized theory and, in addition, provides a check on the correctness of the hydrofoil-airfoil equivalence results.

THE FLAPPED-PLATE HYDROFOIL

Because of its usefulness as a control surface, the configuration consisting of a hydrofoil with a hinged or flapped after portion is of particular interest. As a particular case, and one revealing the effect of the flap size on the flap effectiveness, the flapped-plate hydrofoil, as shown schematically in Figure 7, will be discussed.

It follows from Equations [17] and [18] that

$$A_0 = \epsilon \left(\frac{\pi - \theta_k}{\pi} \right) \quad [21]$$

$$A_k = \frac{2\epsilon}{\pi\alpha} \sin \alpha \theta_k \quad [22]$$

where

$$\frac{\theta_k}{s} = \frac{1}{2}(1 - \cos \theta_k) \cdot \sqrt{\frac{z_k}{s}} \quad [23]$$

CONFIDENTIAL

CONFIDENTIAL

11

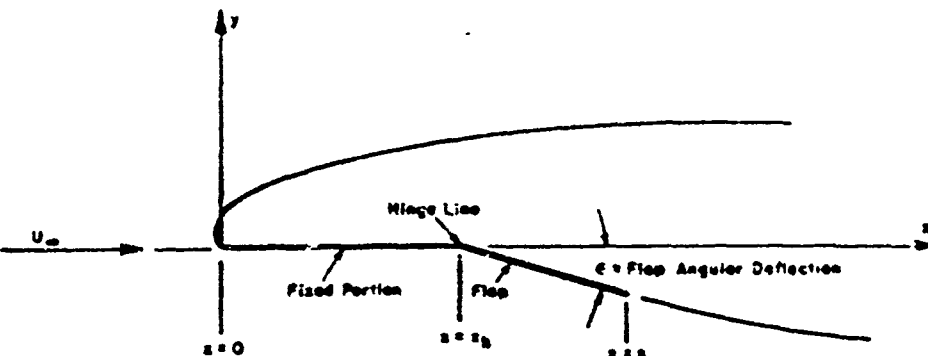


Figure 7 - Flapped-Plate Hydrofoil

Then, using Equations [A3], [A4], [A5] and Equations [14], [15], [16],

$$C_L = \bar{C}_L = \frac{\pi}{2} \left(A_0 + A_1 - \frac{A_2}{2} \right) = \frac{\epsilon}{2} [x - \theta_b + \sin \theta_b (2 - \cos \theta_b)] \quad (24)$$

$$\begin{aligned} C_M = \bar{C}_{M_3} &= \frac{\pi}{32} \left(5A_0 + 7A_1 - 7A_2 + 3A_3 - \frac{A_4}{2} \right) \\ &= \frac{\epsilon}{32} [5(x - \theta_b) + 14 \sin \theta_b - 7 \sin 2\theta_b + 2 \sin 3\theta_b - \frac{1}{4} \sin 4\theta_b] \end{aligned} \quad (25)$$

$$C_D = \frac{1}{8\pi} \bar{C}_L^2 = \frac{\pi}{2} \left(A_0 + \frac{A_1}{2} \right)^2 = \frac{\epsilon^2}{2\pi} [x - \theta_b + \sin \theta_b]^2 \quad (26)$$

The quantities $(dC_L)/(de)$ and $(dC_M)/(de)$ are shown as a function of flap chord ratio in Figure 8. It is important to note that the lift effectiveness of all flaps larger than 41 percent chord is as great as or greater than the lift effectiveness of an unflapped foil. A 75 percent flap, for which the lift effectiveness is an optimum, has a lift effectiveness 114 percent of the unflapped foil effectiveness. This is in contrast with the situation for noncavitating airfoils, for which the flap effectiveness continually increases with increasing flap chord ratio.

The lift/drag ratio of a flapped foil for a given lift coefficient is greater the smaller the flap chord ratio. In Figure 9 this ratio is shown as a function of lift coefficient for an unflapped plate and for a 25 percent flapped plate for which $L/D = 5.21 C_L$. The flapped plate is seen to be decidedly superior. It is an important result, demonstrated by this example, that the cavitation drag of a hydrofoil operating at a given lift coefficient is very much dependent on the hydrofoil shape.

CONFIDENTIAL

CONFIDENTIAL

12

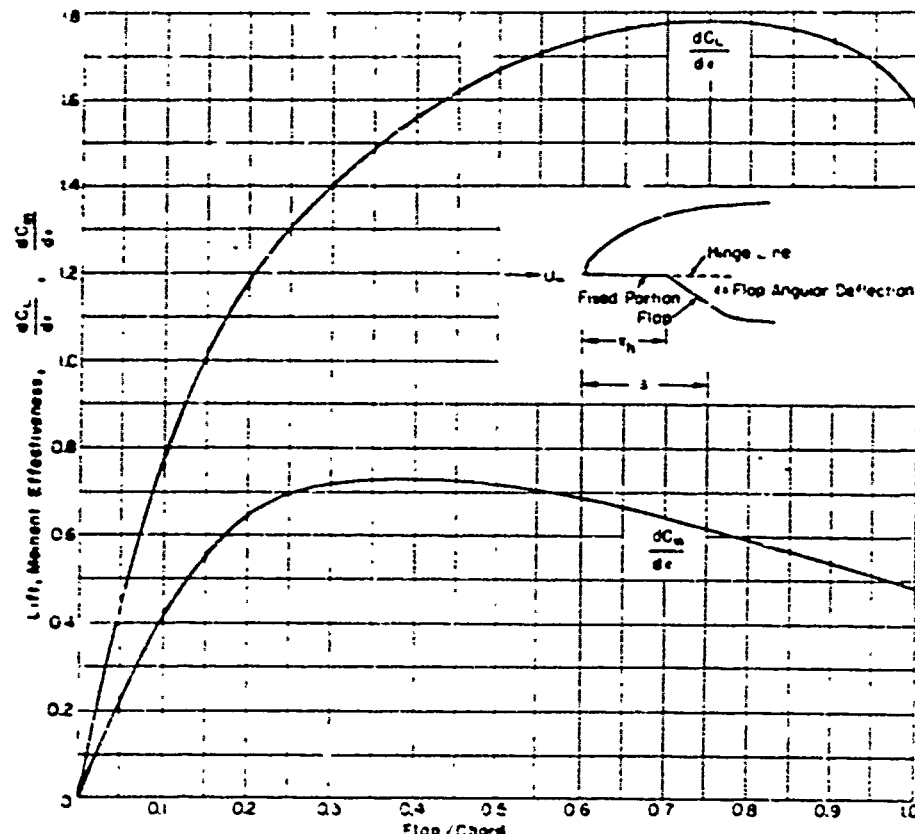


Figure 5 - Lift and Moment Effectiveness for Flapped-Plate Hydrofoil

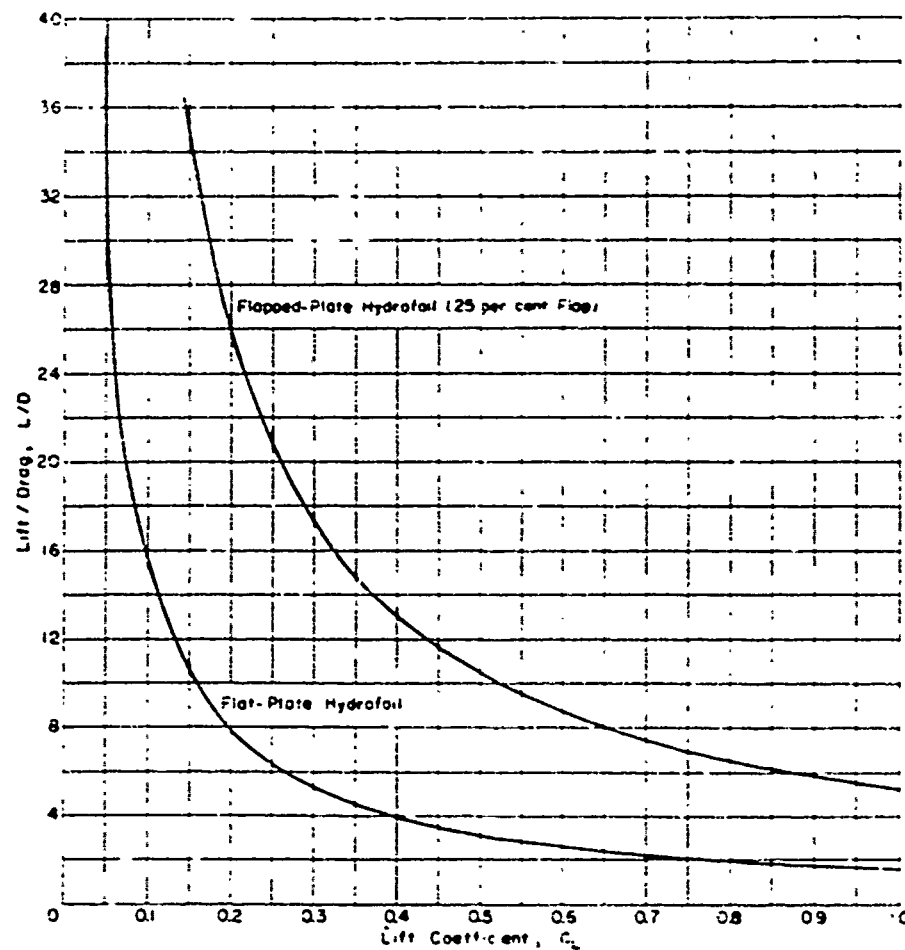
LOW-DRAG HYDROFOILS

The specification of hydrofoils with low cavitation drag is a problem of great practical importance. Because the drag may be several times larger than necessary on an improperly designed configuration, the success of high-speed hydrofoil boats and, particularly, supercavitating screws may well depend upon the proper choice of the hydrofoil sections.

It is of interest first to determine the minimum C_D (the lift coefficient being specified) for the class of all possible cavitating hydrofoils. In view of the hydrofoil-airfoil equivalence, the problem becomes one of determining the minimum C_L (the moment coefficient being specified) for the class of all possible airfoils on whose lower surface the pressure is nowhere

CONFIDENTIAL

CONFIDENTIAL

Figure 3 - L/D vs. C_L for Flat-Plate and Flapped-Plate Hydrofoils

less than the free stream pressure. Low drag equivalent airfoils will thus have centers of pressure relatively far aft of the leading edge. The optimum airfoil pressure distribution can be immediately specified. It is shown in Figure 10 where $\delta(\bar{x})$ is the Dirac delta function defined such that

$$\int \delta(\bar{x} - \bar{x}_1) d\bar{x} = 1 \text{ and } \delta(\bar{x} - \bar{x}_1) = 0 \text{ for } \bar{x} \neq \bar{x}_1$$

The question of the practical possibility of obtaining such a pressure distribution need not be considered. The important thing is that this case does furnish a lower bound for the hydrofoil drag which may be used as a measure of drag performance.

CONFIDENTIAL

CONFIDENTIAL

14

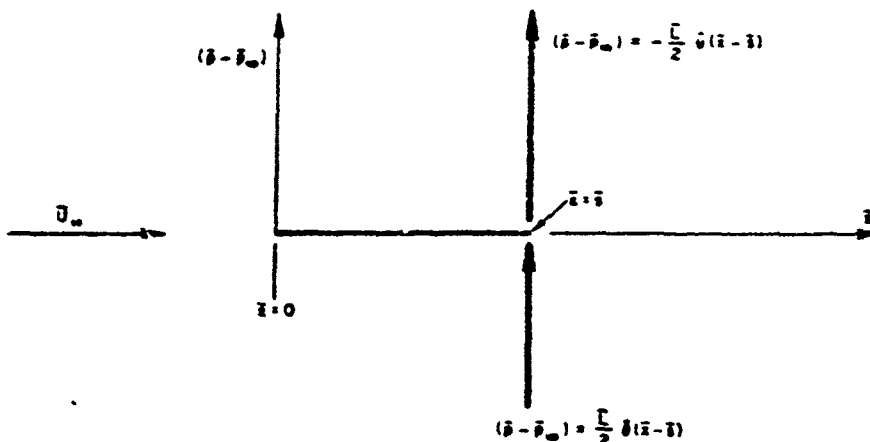


Figure 10 - Optimum Low-Drag Pressure Distribution on Equivalent Airfoil

For this optimum pressure distribution,

$$\bar{C}_D = \frac{N}{\frac{1}{2} \rho \bar{U}_\infty^2 \bar{s}^2} = \frac{\bar{s} \bar{L}}{\frac{1}{2} \rho \bar{U}_\infty^2 \bar{s}^2} = \bar{C}_L \quad [27]$$

Then,

$$C_L = \bar{C}_L \quad [28]$$

$$C_D = \frac{1}{3\pi} \bar{C}_L^2 \quad [29]$$

$$\left(\frac{C_L}{C_D} \right)_{\text{opt.}} = \frac{8\pi}{C_L} \quad [30]$$

This optimum may be compared to the lift, drag ratio of the flat plate, which, as has already been indicated, is an inferior section.

$$\left(\frac{C_L}{C_D} \right)_{\text{flat plate}} = \frac{\bar{s}}{2\bar{C}_L} \quad [31]$$

It is of importance now to specify a family of hydrofoil sections with relatively low-drag characteristics. Such a family is one whose equivalent airfoil family is described by

$$\frac{d\bar{z}_0}{d\bar{x}} = A_1 \left(\cos \theta - \frac{1}{2} \cos 2\theta \right) = \frac{A_1}{2} \left[1 + \frac{4\bar{x}}{\bar{s}} - 8 \left(\frac{\bar{x}}{\bar{s}} \right)^2 \right] \quad [32]$$

These shapes were chosen from a more general family in such a way that they have a minimum drag and still have pressure distributions such that the bottom pressures are at no

CONFIDENTIAL

CONFIDENTIAL

at less than the free stream pressure. The general family dealt with is one for which the equivalent airfoil family consists of shapes such that $d\bar{y}_0/d\bar{x} = -A_0 + A_1 \cos \theta + A_2 \cos 2\theta$ (see Equation (A6), Appendix A).

For these low-drag shapes,

$$\bar{C}_L = \pi A_1 \quad [33]$$

$$\bar{C}_M = \frac{\pi \pi A_1}{8} \quad [34]$$

$$\bar{C}_{M_3} = \frac{21 \pi A_1}{64} \quad [35]$$

The shape of the corresponding hydrofoil family is

$$\frac{dy_0}{dx} = \frac{A_1}{2} \left(1 + 4\sqrt{\frac{2}{s}} - 8\frac{z}{s} \right) \quad [36]$$

or

$$\frac{y_0}{s} = \frac{A_1}{2} \left[\frac{z}{s} + \frac{8}{3} \left(\frac{z}{s} \right)^{3/2} - 4 \left(\frac{z}{s} \right)^2 \right] \quad [37]$$

for which

$$C_L = \bar{C}_M = \frac{\pi \pi A_1}{8} \quad [38]$$

$$C_M = \bar{C}_{M_3} = \frac{21 \pi A_1}{64} \quad [39]$$

$$C_D = \frac{1}{8\pi} (\bar{C}_L)^2 = \frac{\pi A_1^2}{8} \quad [40]$$

$$\frac{C_L}{C_D} = \frac{25 \pi}{8 C_L} \text{ (when operating at design } C_L) \quad [41]$$

Equation (17) may be rewritten

$$\frac{y_0}{s} = \frac{4 C_{L_d}}{5\pi} \left[\left(\frac{z}{s} \right) + \frac{8}{3} \left(\frac{z}{s} \right)^{3/2} - 4 \left(\frac{z}{s} \right)^2 \right] \quad [37a]$$

where C_{L_d} is the design lift coefficient. The shape of these sections is shown in Fig. 11 where $(y_0/s)/(4 C_{L_d}/5\pi)$ is plotted as a function of (z/s) .

Comparison of the drag characteristics of these low-drag airfoils with those of a flat plate reveal that for a given lift coefficient they have only one sixth the drag of a flat plate. Comparison with the optimum case (Equation (30)) indicates that even this low-drag family may be improved upon. Such a development is not to be attempted here.

CONFIDENTIAL

CONFIDENTIAL

16

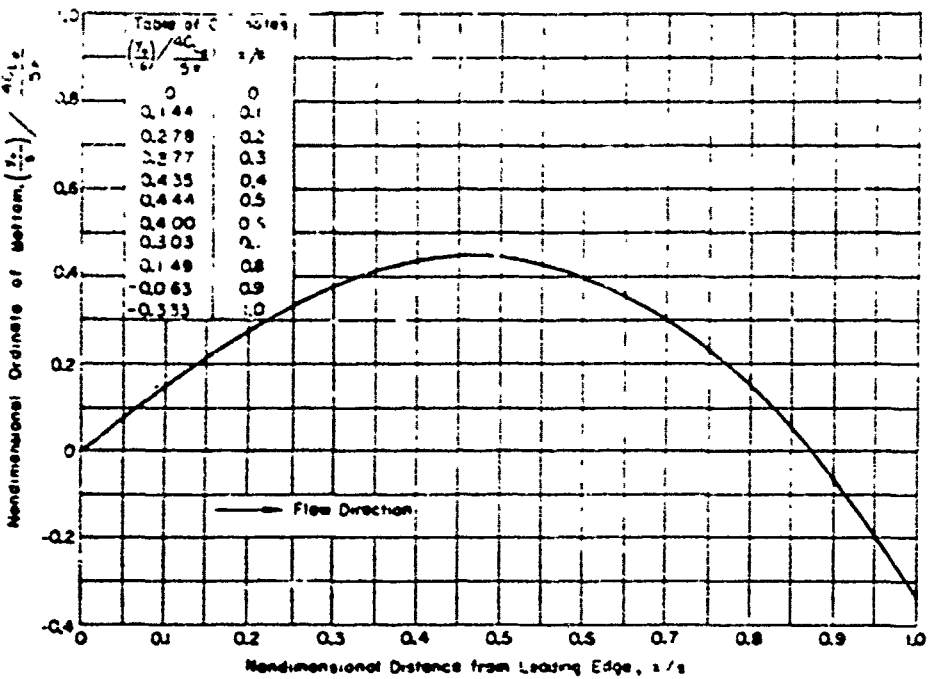


Figure 11 - Low-Drag Hydrofoil Sections

It is to be noted that the lift/drag ratio calculated (Equation [41]) is only obtained when the foil is operating at its design lift coefficient, for which, incidentally, the flow enters the leading edge without stagnating (so-called "shock-free" entry). For angles of attack less than the design angle, the foil will probably cavitate on the lower side and the lift will probably be reversed. It may thus be desirable to operate a foil at some angle of attack slightly larger than the design angle. For such a case it may be shown that

$$\frac{C_L}{C_D} = \frac{\pi}{2} \frac{\frac{C_L}{\alpha' + \frac{3}{5} C_{L_d}}}{\left(C_L - \frac{3}{5} C_{L_d} \right)^2} = \frac{\alpha' + \frac{3}{5} C_{L_d}}{\left(\alpha' + \frac{1}{5} C_{L_d} \right)^2} \quad [42]$$

where α' is the difference between the operating angle of attack and the design angle of attack. These ratios are shown for several members of the low-drag family in Figure 12. Large increases in drag result when foils are operated at angles of attack substantially larger than the design angles. Nevertheless, cavitation drags equal to or even less than the magnitude of the viscous drag of one wetted surface can probably be obtained in a practical design. Thus, from the drag point of view, supercavitating configurations may be designed with characteristics not inferior to those of noncavitating configurations.

CONFIDENTIAL

CONFIDENTIAL

17

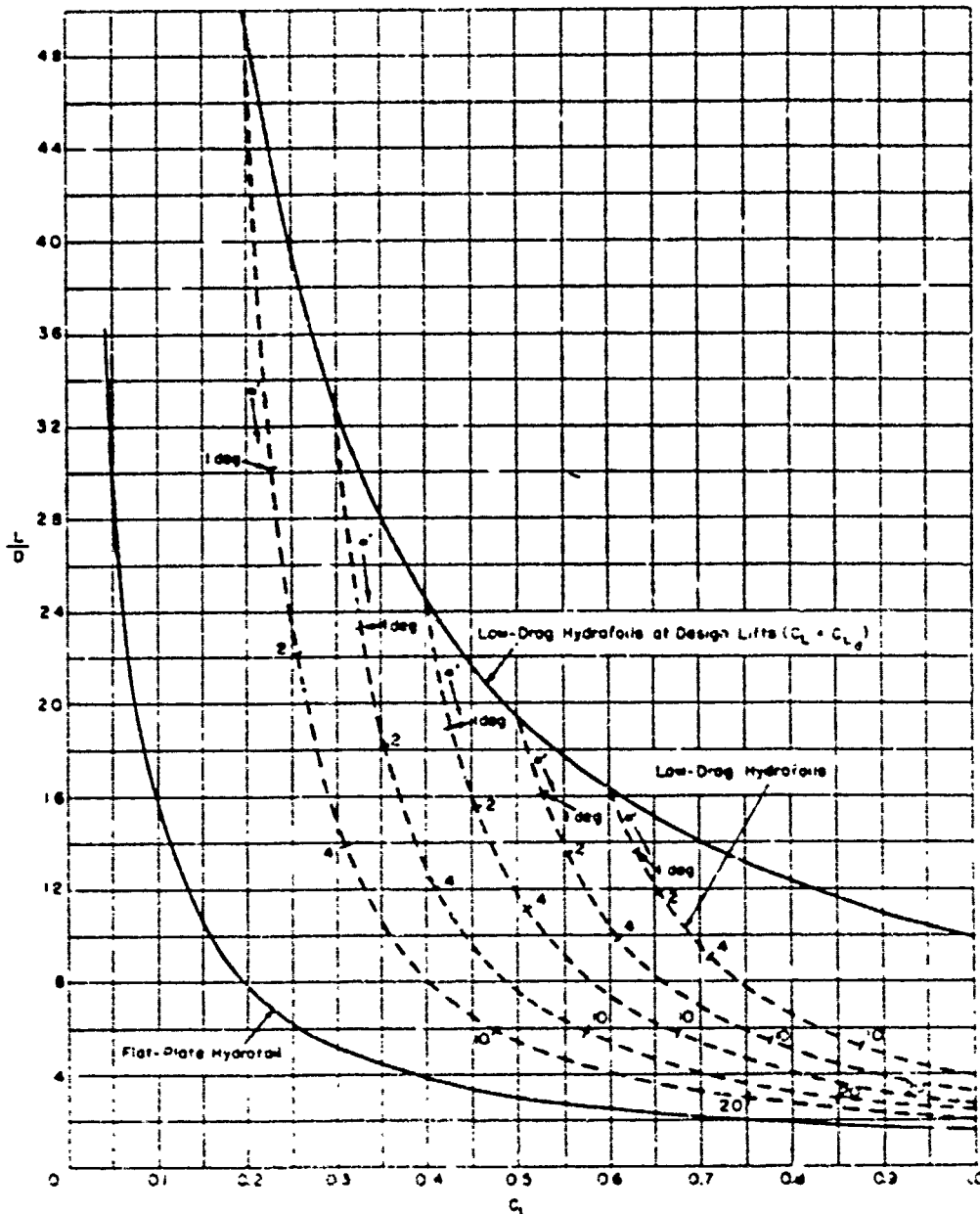


Figure 12 - L/D vs C_L for Low-Drag Hydrofoil Family

CONFIDENTIAL

CONFIDENTIAL

18

SUMMARY

1. The linearized theory is a meaningful first-order theory for calculating the characteristics of supercavitating hydrofoils at small angles of attack. The justification for this conclusion lies in the result that in the case of a flat plate at zero cavitation number, the linearized result for cavity shape, foil forces, and pitching moment is actually the first-order term in an expansion of the exact solution in powers of the angle of attack.
2. The problem of determining the zero cavitation number characteristics of an arbitrary hydrofoil section can be reduced in a simple manner to an equivalent thin airfoil problem. Simple relationships exist between the lift, drag, and pitching moment of the hydrofoil, and the moment, lift, and third moment of the equivalent airfoil. Effective and practical existing methods may be used to solve the thin airfoil problem.
3. The lift curve and moment curve slopes for a flat plate at zero cavitation number are, respectively, $\pi/2$ and $5\pi/32$, as compared with the corresponding values for the noncavitating flat plate of π and $\pi/2$. These values also represent the lift and moment effectiveness with respect to angle of attack of cambered sections.
4. At zero cavitation number, the lift effectiveness (with respect to flap deflection) of all flaps larger than 41 percent chord is as great or greater than the lift effectiveness of an unflapped foil (flat plate).
5. The cavitation drag accompanying a given lift is very much dependent on the hydrofoil shape. An absolute minimum drag exists for any given lift. All practical hydrofoils must have drags larger than this absolute minimum, which is $(C_D)_{\text{min}} = (C_L)^2/8\pi$.
6. For all size flaps, the generation of lift by flap deflection results in less drag than the generation of lift by angle of attack changes. Thus, from the cavitation drag standpoint, the flat plate is an inferior hydrofoil section.
7. The generation of lift by the proper use of camber results in less drag than the generation of lift by flap deflection for practical size flaps.
8. Cambered hydrofoils may be designed for drag operation, for which the cavitation drag at moderate lift coefficients is approximately the same as the viscous drag of one wetted surface. Thus, supercavitating configurations may probably be designed with drag characteristics not essentially inferior to those of noncavitating configurations.
9. A family of relatively low-drag hydrofoils and their theoretical characteristics are presented in the present paper.

CONFIDENTIAL

CONFIDENTIAL

APPENDIX A

USEFUL RESULTS OF THE LINEARIZED AIRFOIL THEORY

The notation of Figure 2 will be used; in particular, the airfoil ordinate $\bar{y}_0(\bar{x})$ is measured normal to the free stream direction. This notation differs from that of Glauert (Reference 4, Chapter VII) where the airfoil ordinate is measured normal to the chord line and accounts for those differences between the presentation below and that of Glauert.

If

$$\bar{x} = \frac{\bar{z}}{2}(1 - \cos \theta) \quad [1]$$

and it is assumed that

$$\bar{u}(\bar{x}, 0+) = \bar{U}_{\infty} \left\{ A_0 \cos \frac{\theta}{2} + \sum_{n=1}^{\infty} A_n \sin n\theta \right\} \quad [2]$$

then it follows that

$$\bar{C}_L = \frac{\bar{L}}{\frac{1}{2} \rho \bar{U}_{\infty}^2 \bar{x}} = \frac{\pi}{2} \left(A_0 + \frac{A_1}{2} \right) \quad [A3]$$

$$\bar{C}_M = \frac{\bar{M}}{\frac{1}{2} \rho \bar{U}_{\infty}^2 \bar{x}^2} = \frac{\pi}{2} \left(A_0 + A_1 - \frac{A_2}{2} \right) \quad [A4]$$

$$\bar{C}_{M_3} = \frac{\bar{M}_3}{\frac{1}{2} \rho \bar{U}_{\infty}^2 \bar{x}^4} = \frac{\pi}{32} \left(5A_0 + 7A_1 - 7A_2 + 3A_3 - \frac{A_4}{2} \right) \quad [A5]$$

It also follows from Equation [4] that

$$\frac{d\bar{y}_0}{d\bar{x}}(\theta) = -A_0 + \sum_{n=1}^{\infty} A_n \cos n\theta \quad [A6]$$

where

$$A_0 = -\frac{1}{\pi} \int_0^{\pi} \frac{d\bar{y}_0}{d\bar{x}}(\theta) d\theta \quad [A7]$$

$$A_n = \frac{2}{\pi} \int_0^{\pi} \frac{d\bar{y}_0}{d\bar{x}}(\theta) \cos n\theta d\theta \quad [A8]$$

The thin airfoil shape being given, the above relations permit the calculation of pressure distribution and resultant forces and moments.

CONFIDENTIAL

APPENDIX B

WAKE SHAPE ACCORDING TO LINEARIZED AND EXACT THEORIES

LINEARIZED THEORY

According to the assumptions of the linearized theory and using the notation of Figure 1,

$$\frac{dy_e \text{ (upper; } z)}{dz} = \frac{v(z, 0+)}{U_\infty} \quad [B1]$$

$$\frac{dy_e \text{ (lower; } z)}{dz} = \frac{v(z, 0-)}{U_\infty}$$

from which it follows

$$y_e \text{ (upper; } z) = \frac{1}{U_\infty} \int_0^z v(t, 0+) dt \quad [B2]$$

$$y_e \text{ (lower; } z) = \frac{1}{U_\infty} \int_0^z v(t, 0-) dt$$

The problem of finding $v(t, 0+)$ and $v(t, 0-)$ for the hydrofoil may be transformed into the problem of finding $\bar{v}(\tilde{t}, 0)$ in the airfoil plane. Making use of the transformation, Equation [5], Equation [B2] then becomes

$$y_e \text{ (upper; } z) = \frac{2}{U_\infty} \int_0^{\tilde{z}=\sqrt{z}} \bar{v}(\tilde{t}, 0) \tilde{t} d\tilde{t} \quad [B3]$$

$$y_e \text{ (lower; } z) = \frac{2}{U_\infty} \int_0^{\tilde{z}=\sqrt{z}} \bar{v}(\tilde{t}, 0) \tilde{t} d\tilde{t}$$

The problem of finding $\bar{v}(\tilde{t}, 0)$ for a flat-plate airfoil of unit chord a ; angle of attack α may be solved by a mapping technique. The image of the \tilde{z} -axis in the conjugate complex velocity plane is a polygon (see Figure B1). It may be mapped onto its image in the physical plane by making use of a Schwarz-Christoffel transformation. The mapping function is then the solution of the present problem since it provides a relation between the velocity components and the physical space coordinates.

As the polygon in the complex velocity plane is traversed from B to C to D to A to B , the region on the right is to be transformed into the lower half of the physical plane. The vertices of the polygon $BCDAB$ are to be mapped into the points 0 and 1 in the physical plane. The interior angle at C is $\pi/2$; the interior angle at B is $-\pi/2$. The mapping function is then:

$$\frac{dz}{d\zeta} = \frac{A}{\zeta^{3/2} \sqrt{\zeta - 1}} \quad [B4]$$

CONFIDENTIAL

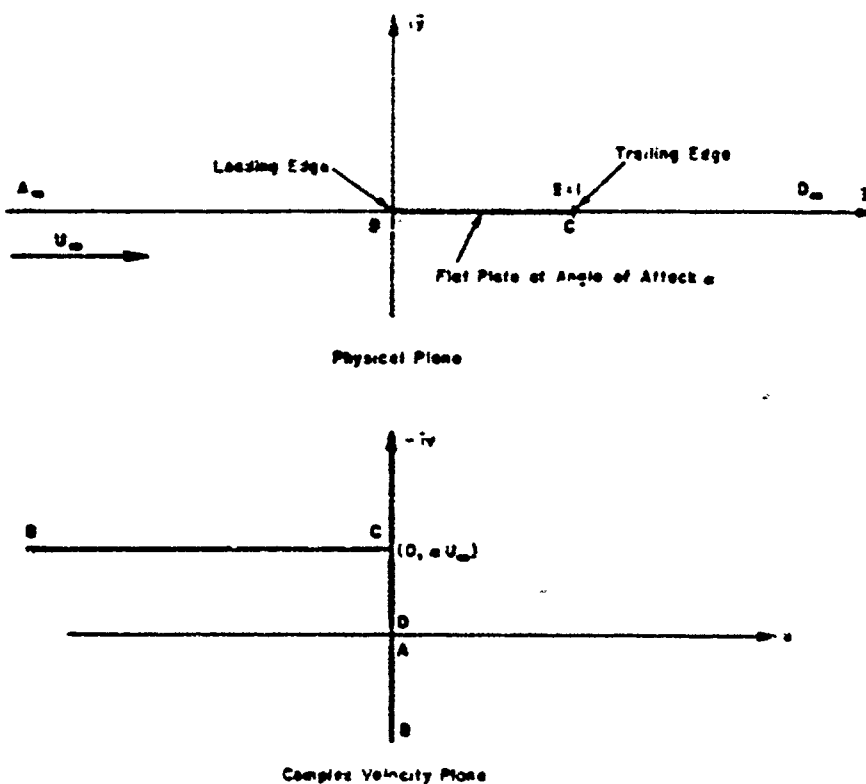


Figure B1 - Flat Plate Airfoil in Physical and Complex Velocity Planes

or

$$v = 2A \sqrt{\frac{\zeta-1}{\zeta}} + B \quad [B5]$$

The constants A and B are determined so that $v(1, 0) = U_{\infty} \alpha i$ and $v(\infty) = 0$. Then

$$v = U_{\infty} \alpha i \left[1 - \sqrt{\frac{\zeta-1}{\zeta}} \right] \quad [B6]$$

Thus

$$v(\bar{z}, 0) = -U_{\infty} \alpha i \left[1 - \sqrt{\frac{\bar{z}-1}{\bar{z}}} \right], \quad \bar{z} < 0$$

$$v(\bar{z}, 0) = -U_{\infty} \alpha i, \quad 0 < \bar{z} < 1 \quad [B7]$$

$$v(\bar{z}, 0) = -U_{\infty} \alpha i \left[1 - \sqrt{\frac{\bar{z}-1}{\bar{z}}} \right], \quad \bar{z} > 1$$

CONFIDENTIAL

CONFIDENTIAL

52

Substituting Equation [B7] in [B3],

$$y_e(\text{upper; } z) = \alpha \left[-z + \frac{1}{2}(1+2\sqrt{2}) \sqrt{z+\sqrt{z}} + \frac{1}{4} \ln \left(1+2\sqrt{z}-2\sqrt{z+\sqrt{z}} \right) \right], z > 0$$

$$y_e(\text{lower; } z) = -\alpha z, \quad 0 < z < 1 \quad [\text{B8}]$$

$$x_e(\text{lower; } z) = \alpha \left[-z - \frac{1}{2}(1-2\sqrt{2}) \sqrt{z-\sqrt{z}} - \frac{1}{4} \ln \left(-1+2\sqrt{z}+2\sqrt{z-\sqrt{z}} \right) \right], z > 1$$

EXACT THEORY

The exact wake shape in parametric form is easily found by making use of the results of the exact solution as presented in Reference 2, Chapter XII.

In the present notation and assuming a plate of unit chord,

$$\begin{aligned} z_e &= -\frac{\cos \alpha}{2} \left[\zeta_1 - \frac{\cos \alpha}{2} (\zeta_1^2 - 1) - 1 \right] \\ &\quad + \frac{\sin^2 \alpha}{4} \left[\zeta_1 \sqrt{\zeta_1^2 - 1} - \ln \left(\zeta_1 + \sqrt{\zeta_1^2 - 1} \right) \right], \quad 1 < \zeta_1 < -1 \end{aligned} \quad [\text{B9}]$$

$$\begin{aligned} y_e(\text{upper}) &= \frac{\sin \alpha}{2} \left[\zeta_1 - \frac{\cos \alpha}{2} (\zeta_1^2 - 1) - 1 \right] \\ &\quad + \frac{\sin \alpha \cos \alpha}{4} \left[\zeta_1 \sqrt{\zeta_1^2 - 1} + \ln \left(\zeta_1 - \sqrt{\zeta_1^2 - 1} \right) \right], \quad 1 < \zeta_1 \end{aligned} \quad [\text{B10}]$$

$$\begin{aligned} y_e(\text{lower}) &= \frac{\sin \alpha}{2} \left[\zeta_1 - \frac{\cos \alpha}{2} (\zeta_1^2 - 1) - 1 \right] \\ &\quad - \frac{\sin \alpha \cos \alpha}{4} \left[\zeta_1 \sqrt{\zeta_1^2 - 1} + \ln \left(-\zeta_1 + \sqrt{\zeta_1^2 - 1} \right) \right], \quad \zeta_1 < -1 \end{aligned} \quad [\text{B11}]$$

where ζ_1 is a parameter.

Expanding Equations [B9], [B10], and [B11] in a power series in the angle of attack,

$$z_e = -\frac{1}{2} \left[\zeta_1 - \frac{1}{2} \zeta_1^2 - \frac{1}{2} \right] + O(\alpha^2), \quad 1 < \zeta_1 < -1 \quad [\text{B12}]$$

$$\begin{aligned} y_e(\text{upper}) &= \frac{\alpha}{2} \left[\zeta_1 - \frac{1}{2} \zeta_1^2 - \frac{1}{2} \right] + \frac{\alpha}{4} \left[\zeta_1 \sqrt{\zeta_1^2 - 1} - \ln \left(\zeta_1 - \sqrt{\zeta_1^2 - 1} \right) \right] \\ &\quad + O(\alpha^3), \quad 1 < \zeta_1 \end{aligned} \quad [\text{B13}]$$

$$\begin{aligned} y_e(\text{lower}) &= \frac{\alpha}{2} \left[\zeta_1 - \frac{1}{2} \zeta_1^2 - \frac{1}{2} \right] - \frac{\alpha}{4} \left[\zeta_1 \sqrt{\zeta_1^2 - 1} + \ln \left(-\zeta_1 + \sqrt{\zeta_1^2 - 1} \right) \right] \\ &\quad + O(\alpha^3), \quad \zeta_1 < -1 \end{aligned} \quad [\text{B14}]$$

CONFIDENTIAL

CONFIDENTIAL

Finally, upon elimination of the parameter ζ_1 from Equations [B12] - [B14], the following result is obtained

$$y_e(\text{exact}) = y_e(\text{linearized}) + O(\alpha^2) \quad [\text{B } 15]$$

where $y_e(\text{linearized})$ is given in Equation [B8].

CONFIDENTIAL

CONFIDENTIAL

24

APPENDIX C
LISTING OF USEFUL THEORETICAL RESULTS

For convenience, the most useful theoretical results are listed below:

Relationship between hydrofoil shape and equivalent airfoil shape:

$$\frac{dy_0}{ds}(s) = \frac{\bar{y}_0}{\bar{s}}(\sqrt{s}) \quad [6]$$

Relationships between hydrofoil forces and moments, and equivalent airfoil forces and moments:

$$C_L = \bar{C}_M \quad [14]$$

$$C_M = \bar{C}_{M_3} \quad [15]$$

$$C_D = \frac{1}{3\pi} \bar{C}_L^2 \quad [16]$$

Forces, pitching moment about leading edge, and lift/drag ratio for a flat-plate hydrofoil ($\sigma = 0$):

$$C_L = \frac{\pi\alpha}{2} \quad [17a]$$

$$C_M = \frac{5\pi\alpha}{32} \quad [18a]$$

$$C_D = \frac{\pi\alpha^2}{2} \quad [19a]$$

$$L/D = \frac{\pi}{2\bar{C}_L} \quad [31]$$

Forces and pitching moment about leading edge for a flapped-plate hydrofoil ($\sigma = 0$) (see Figure 7):

$$C_L = \frac{\epsilon}{2} [\pi - \theta_A + \sin \theta_A (2 - \cos \theta_A)] \quad [24]$$

$$C_M = \frac{\epsilon}{32} \left[5(\pi - \theta_A) + 14 \sin \theta_A - 7 \sin 2\theta_A + 2 \sin 3\theta_A - \frac{1}{4} \sin 4\theta_A \right] \quad [25]$$

$$C_D = \frac{\epsilon^2}{2\pi} (\pi - \theta_A + \sin \theta_A)^2 \quad [26]$$

where

$$\sqrt{\frac{\theta_A}{s}} = \frac{1}{2}(1 - \cos \theta_A) \quad [23]$$

Optimum hydrofoil lift/drag ratio ($\sigma = 0$):

$$\left(\frac{L}{D} \right)_{opt} = \frac{8\pi}{C_L} \quad [21]$$

CONFIDENTIAL

CONFIDENTIAL

Lift/drag ratio for relatively low-drag hydrofoils ($\sigma = 0$) (see Figure 11):

$$\frac{L}{D} = \frac{\alpha' + \frac{2}{\pi} C_{L_d}}{\left(\alpha' + \frac{4}{5\pi} C_{L_d} \right)^2} \quad [42]$$

where C_{L_d} is the design lift coefficient and α' is the difference between the operating angle of attack and the design angle of attack.

REFERENCES

1. Batchelor, G., "Hydrodynamics," Princeton University Press for University of Cincinnati (1950).
2. Milne-Thomson, L.M., "Theoretical Hydrodynamics," Second Edition, The Macmillan Company, New York (1950).
3. Tulin, M.P., "Steady Two-Dimensional Cavity Flows About Slender Bodies," David Taylor Model Basin Report 834 (May 1953).
4. Glauert, H., "The Elements of Aerofoil and Airscrew Theory," The Macmillan Company, New York (1944).
5. Lamb, H., "Hydrodynamics," Sixth Edition, Dover Publications, New York (1945).

CONFIDENTIAL

UNCLASSIFIED

27

INITIAL DISTRIBUTION

Source	Source	Source
1-21 Chief, Battles, Library (Code 112) 1-5 Tech Library 6 Tech Acc to Chief (Code 351) 7 Tech Info Directorate (Code 351) 8-A Areas, Area Inv of New Arca 8-B Bus & Dev (Code 351) 10 Applied Sciences (Code 351) 11 Areas, Areas, & Inv Br (Code 370) 12 Bus Servs (Code 450) 13-16 Power Inv & Inv Pts (Code 450) 15 Public Relations (Code 471) 16 Astronaut License (Code 523) 17 Guidance Design (Code 450) 18 Instrumentation (Code 520) 19 Instrumentation (Code 520) 20 Technical Communication (Code 330-8) 21 Propulsion & Stability (Code 354)	52 DIR, Appl Physics Div, Sandia Corp., Albuquerque, N.M., no REC'D, Fund Contract AF-TPR 64 Chief, Hydromech Div Br, TVA, Knoxville, Tenn. 65-66 210, Tech Inv Br, Aerospace Prevee Group, Mountain, Md. 67 CO, Transportation Inv & Dev Div, Fort Eustis, Va. 68 DIR, Appl Physics Lab, Jones Space Inv, Silver Spring, Md., no REC'D 69 Subcontractors (Code 450) 70 Battelle Steel Co., Research Div, Jersey, N.J., no SUPPLYPRSCD 71 Battelle Inv Div, Batt, Md., no SUPPLYPRSCD 72 Battelle Aerospace Corp., Tewksbury, R.I., no REC'D 73 212, Space Lab, CIT, Pasadena, Calif., no REC'DAT, Los Angeles, Calif. 74 DIR, Science Inst of Oceanography, Univ of Calif., La Jolla, Calif., no REC'D, Pasadena, Calif. 75 General Electric Co., Schenectady, N.Y., no REC'D 76 Human Lab, Cedar Ferry, N.Y., no REC'D, See Tech 77 DIR, Acoustics Lab, MIT, Cambridge, Mass., no REC'D, Boston, Mass., no SUPPLYPRSCD, Boston 78 Head, Div of SAME, MIT, Cambridge, Mass., no REC'D, Boston, Mass. 79-80 Export News Bldg & Dry Dock Co., Newport News, Va., no SUPPLYPRSCD 79 212 Inv Inv 80 Inv, Dynamic Lab 81 New Port Shipping Corp., Camden, N.J., no SUPPLYPRSCD 82 CDR, Philadelphia Naval Supply (Code 350) 83 CDR, SURASDEVDET, Key Bisc, Fla. 84-87 CTF, CTFNL (Standby Inv) 88 CDR, USNRL 89-90 CDR, CTF-OTS, Pasadena, Calif. 91 CO & CDR, VSEL, San Diego, Calif. 92 CO & CDR, VSEL, San Diego, Calif. 93 CO & CDR, VSEL, San Diego, Calif. 94 CO & CDR, VSEL, VSEL, Amherst, Mass. 95 CO, CDRNS, Boston, R.I. 96 Astr Inv of Defense Inv & Dev (Code 300) 97 The Director, Warrendale Super Inv, Corps of Engns, PA Army, Warrendale, Penn. 98 DIR, Areas Inv Inv, Langley Field, Calif. 99 DIR, Langley Inv Inv, Langley Field, Va. 100 CDR, Areas Flight Inv Inv, Cleveland, O. 101 DIR, Inv Inv, NASA, Washington, D.C. 102 DIR, Det 2400 Inv Inv, Det 2400, Inv Inv, Penn.	91 Dr. A. F. "Fido", 4130 W. 10th, Ft. Lauderdale, Calif., no REC'DAT, Los Angeles, Calif. 92 Dr. G. Baker, Loring Inv Inv, Langley Field, Va. 93 Dr. A. Bar, Area Inv Inv, 25400 L. 94 Dr. George C. Marling, Prof, New Arca, 817, Cambridge Blvd., no REC'DAT, Boston, Mass. 95 Mr. J. S. Pashman, Langley Inv Inv, Langley Field, Va. 96 Mr. H. S. Plessel, Inv Inv, CIT, Pasadena, Calif., no REC'DAT, Los Angeles, Calif. 97 Mr. Paul L. Russel, Chief, Inv of Power Inv, 45 Harrison Avenue, Boston, Mass. 98 Dr. J. H. Peterson, CTRL, Power Inv Inv, Shaw College, Pa., no Inv Contract Inv 99 Dr. L. G. Shull, CTR, Dr. Anthony Fazio, Physics Inv Inv, Inv of Wash., Cambridge, Mass., no REC'D, Inv of Wash. 100 Dr. C. R. Sonenberg, Head of Mech Engg, MIT, Cambridge, Mass., no REC'DAT, Boston 101 Mr. F. J. Thompson, Langley Inv Inv, Langley Field, Va. 102 Dr. L. Trifun, MIT, Cambridge, Mass., no REC'DAT, Boston, Mass. 103 Mr. Peter Dezza, Mech Engg Inv Inv, Inv Inv Inv, Cambridge, Mass., no SUPPLYPRSCD, Boston 104 Dr. Howard Ryland, CIT, Pasadena, Calif., no REC'DAT, Los Angeles, Calif. 105 Prof. A. van der Pol, CIT, Pasadena, Calif., no REC'DAT, Los Angeles, Calif. 106 Prof. Lynn S. Jacobson, Head of Mech Engg, Stanford Inv Inv, Calif., no REC'DAT, San Mateo Island, Calif.

UNCLASSIFIED

NOTIFICATION

INSTRUCTIONS: THIS FORM IS FOR
MISSING PAGES

DOCUMENT	UNCLASSIFIED
AD	
ATI	

THE PAGES, FIGURES, CHARTS, PHOTOS

MISSING PAGED BLANK

DO NOT